

Measurements of global and local polarization of hyperons in isobar collisions at 200 GeV from STAR

Xingrui Gou^{1,*}, for the STAR Collaboration

¹Institute of Frontier and Interdisciplinary Science & Key Laboratory of Particle Physics and Particle Irradiation (Ministry of Education), Shandong University, Qingdao, Shandong, 266237, China

Abstract. In heavy-ion collisions, the observation of the global and local polarization of hyperons has revealed the existence of large vorticities perpendicular to reaction plane due to system's orbital angular momentum and along beam direction due to collective velocity field, respectively. With the high-statistics data from isobar collisions of Ru+Ru and Zr+Zr at $\sqrt{s_{NN}} = 200$ GeV collected by the STAR experiment, we present differential measurements of global polarization for $\Lambda/\bar{\Lambda}$ as a function of centrality. These measurements allow us to study the possible magnetic field driven effects through the polarization difference between Ru+Ru and Zr+Zr, owing to a larger magnetic field in the former. Furthermore, the first measurements of Λ hyperon local polarization along beam direction relative to the third-order event plane as well as the second-order event plane are presented. A comparison of results from isobar and Au+Au collisions provides important new insights into the collision system size dependence of the vorticities in heavy-ion collisions.

1 Introduction

In non-central heavy-ion collisions, the produced system has large orbital angular momentum and may have a strong vortical structure, which leads to the global spin polarization of hyperons through the spin-orbital interaction [1]. Due to the nature of the weak decay, Λ hyperon's polarization can be determined through the angular distribution of decay daughter proton in parent's rest frame [1].

Global polarization has been observed for Λ and $\bar{\Lambda}$ hyperons in Au+Au collisions from $\sqrt{s_{NN}} = 7.7$ to 200 GeV by the STAR experiment [2, 4]. Significant global polarization of $\Lambda(\bar{\Lambda})$ observed from low to high energy is consistent with the expectation from the spin-orbit coupling picture, which can be described by hydrodynamic models. Some models predict a system size dependence of global polarization [3, 5]. Experimentally, the system size dependence can be studied by comparing results in isobar collisions with those in Au+Au collisions. Furthermore, the magnetic field effects may cause a splitting between Λ and $\bar{\Lambda}$ global polarization, and initial magnetic field difference between Ru+Ru and Zr+Zr collision may lead to different Λ global polarization in the two systems.

On the other hand, STAR has measured the local polarization with respect to the second-order event plane in Au+Au collisions at $\sqrt{s_{NN}} = 200$ GeV [7]. The local polarization as a function of azimuthal angle relative to the second-order event plane shows a sine modulation,

*e-mail: xgou@rcf.thic.bnl.gov; xingruigou@mail.sdu.edu.cn

as expected from quadrupole structure of vorticity along the beam direction [7]. With high statistics isobar data, measurements of local polarization in smaller systems and relative to higher harmonic event planes can provide new insights into polarization phenomena.

In these proceedings, we report $\Lambda(\bar{\Lambda})$ global and local polarization as a function of centrality in Ru+Ru and Zr+Zr collisions at $\sqrt{s_{NN}} = 200$ GeV using the data collected by STAR experiment.

2 Global polarization results

In the STAR experiment, the first-order event plane can be determined by Zero Degree Calorimeters with Shower Maximum Detectors (ZDC SMD), the second-order and third-order event planes are determined by the Time Projection Chamber detector (TPC). $\Lambda(\bar{\Lambda})$ hyperons have been reconstructed through its decay channel: $\Lambda \rightarrow \pi^- + p$ ($\bar{\Lambda} \rightarrow \pi^+ + \bar{p}$). The residual background under the mass peak is smaller than 3%. The global polarization is determined by

$$P_{\Lambda} = \frac{8}{\alpha\pi A^0} \frac{\langle \sin(\Psi_1 - \phi_p^*) \rangle}{\text{Res}(\Psi_1)}, \quad (1)$$

where α is the decay parameter, A^0 is the acceptance correction factor, ϕ_p^* is the azimuthal angle of decay proton in Λ s rest fame and $\text{Res}(\Psi_1)$ is the first-order event plane resolution [2].

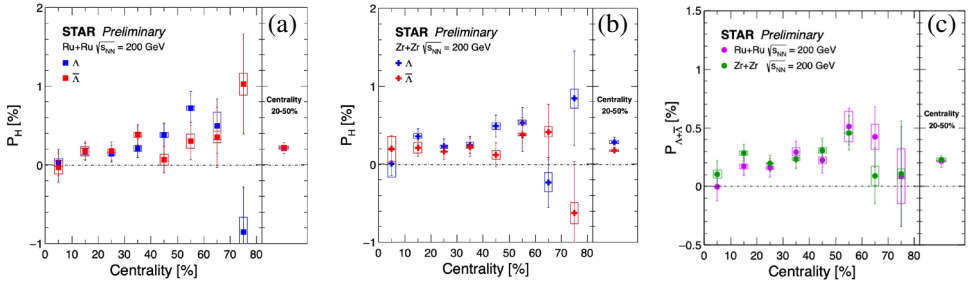


Figure 1: Global polarization of Λ and $\bar{\Lambda}$ as a function of centrality in Ru+Ru(a), Zr+Zr(b) collisions at $\sqrt{s_{NN}} = 200$ GeV. Panel (c) shows $\Lambda+\bar{\Lambda}$ global polarization results in isobar collisions. Open boxes and vertical lines represent systematic and statistical uncertainties.

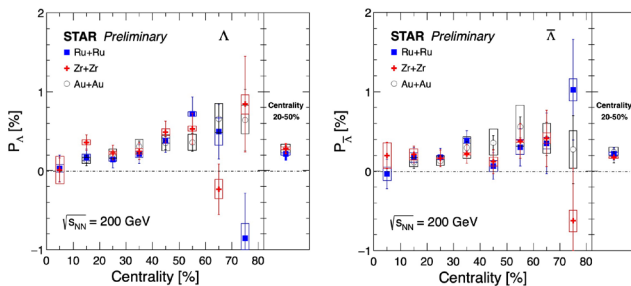


Figure 2: Λ (left) and $\bar{\Lambda}$ (right) global polarization as a function of centrality in Ru+Ru, Zr+Zr, and Au+Au collisions at $\sqrt{s_{NN}} = 200$ GeV.

Figure 1 (a) and (b) show Λ and $\bar{\Lambda}$ global polarization $P_{\Lambda/\bar{\Lambda}}$ as a function of centrality in Ru+Ru and Zr+Zr collisions. The trend of the results increase from central to peripheral

centrality. For better precision, we also combine 20-50% centrality results. No significant difference between Λ and $\bar{\Lambda}$ global polarization in Ru+Ru and Zr+Zr collisions has been observed which indicates that no magnetic field effects on the hyperon polarization is observed in isobar collisions within current statistical limitation.

Figure 1 (right) shows $\Lambda + \bar{\Lambda}$ global polarization $P_{\Lambda + \bar{\Lambda}}$ as a function of centrality in Ru+Ru and Zr+Zr collisions. The results are consistent in each centrality between Ru+Ru and Zr+Zr collisions.

Figure 2 shows Λ and $\bar{\Lambda}$ global polarization comparison between isobar and Au+Au collisions. The results are consistent between isobar and Au+Au collisions for the whole centrality range, indicating there might be little collision system size dependence.

3 Local polarization results

The component of the polarization along the beam direction can be measured by

$$\langle \cos\theta_p^* \rangle = \int \frac{dN}{d\Omega^*} \cos\theta_p^* d\Omega^*, \quad (2)$$

where θ_p^* is the polar angle of the daughter proton in the Λ rest frame [7].

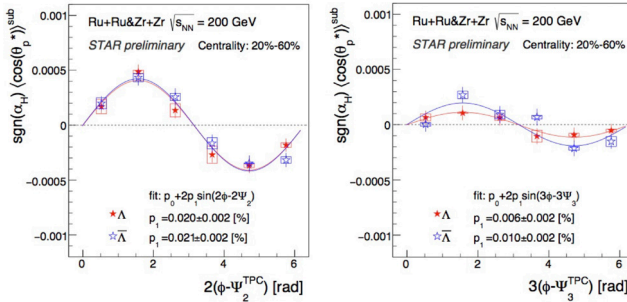


Figure 3: $\langle \cos\theta_p^* \rangle$ of Λ and $\bar{\Lambda}$ hyperons as a function of azimuthal angle ϕ relative to the second-order event plane Ψ_2 (left) and third-order event plane Ψ_3 (right) for 20% – 60% centrality in isobar collisions at $\sqrt{s_{\text{NN}}} = 200$ GeV. $\langle \rangle^{sub}$ denotes the subtraction of the acceptance effect. Solid lines show the fit with the sine function.

Figure 3 shows $\langle \cos\theta_p^* \rangle$ of Λ and $\bar{\Lambda}$ hyperons as a function of azimuthal angle ϕ relative to the second-order event plane Ψ_2 (left) and third-order event plane Ψ_3 (right) for 20% – 60% centrality respectively. The solid lines are the fits to the results with $p_0 + 2p_1 \sin(n\phi - n\Psi_n)$. The signal on Figure 3 (left) shows a clear sine modulation, as expected from quadrupole structure of vorticity along the beam direction. The trend is similar to that in Au+Au collisions. Figure 3 (right) shows the first measurements of $\langle \cos\theta_p^* \rangle$ with respect to the third-order event plane Ψ_3 . The results also show a sine modulation for both Λ and $\bar{\Lambda}$, indicating a v_3 driven polarization.

Figure 4 (left) presents the centrality dependence of the second and third Fourier sine coefficients of the local polarization $\langle P_2 \sin[n(\phi - \Psi_n)] \rangle$. The increase of the results with centrality is in line with the increasing of elliptic flow magnitude towards peripheral collisions. A significant local polarization with respect to the third-order event plane has been observed which increases with centrality. The results show no significant difference between the second-order and third-order local polarization within uncertainties. The hydrodynamic model with a shear term [6] reasonably describes the data for central collisions, but not for the peripheral ones.

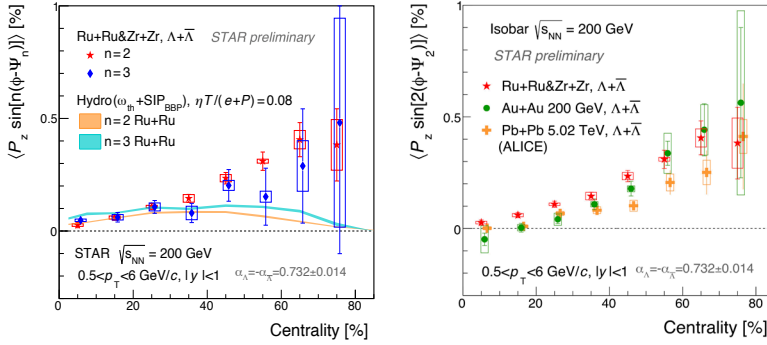


Figure 4: Left: the second and third Fourier sine coefficients of the local polarization of $\Lambda + \bar{\Lambda}$ as a function of the collision centrality in isobar collisions at $\sqrt{s_{NN}} = 200$ GeV. Right: the comparison of the second Fourier sine coefficient of $\Lambda + \bar{\Lambda}$ local polarization among isobar, Au+Au collisions at $\sqrt{s_{NN}} = 200$ GeV and Pb+Pb collisions at $\sqrt{s_{NN}} = 5.02$ TeV.

Figure 4 (right) shows the $\langle P_z \sin [2 (\phi - \Psi_2)] \rangle$ of $\Lambda + \bar{\Lambda}$ local polarization with respect to the second-order event plane as a function of the collision centrality in isobar, Au+Au, and Pb+Pb collisions [8]. A hint of system size dependence has been observed comparing isobar and Au+Au collisions at $\sqrt{s_{NN}} = 200$ GeV, while the energy dependence is not obvious between $\sqrt{s_{NN}} = 200$ GeV Au+Au collisions and $\sqrt{s_{NN}} = 5.02$ TeV Pb+Pb collisions.

4 Summary

The global and local polarizations of Λ and $\bar{\Lambda}$ have been measured in Ru+Ru and Zr+Zr collisions at $\sqrt{s_{NN}} = 200$ GeV. For global polarization, Λ and $\bar{\Lambda}$ results are consistent, showing that the magnetic field effects on global polarization are not observed in isobar collisions within current statistical limitation. Global polarization results are consistent between Ru+Ru, Zr+Zr, and Au+Au collisions. No obvious collision system size dependence is observed. Significant local polarization signals with respect to the second-order and third-order event plane are observed in isobar collisions at $\sqrt{s_{NN}} = 200$ GeV. A slight hint of collision system size dependence has been observed, while energy dependence is not obvious.

Acknowledgements

The author is supported partially by the National Natural Science Foundation of China under No.11890710, No.11890713.

References

- [1] Z. T. Liang and X. N. Wang, Phys. Rev. Lett. 94,102301 (2005); 96, 039901(E) (2006).
- [2] L. Adamczyk et al., (STAR Collaboration), Nature 548, 62 (2017).
- [3] I. Karpenko and F. Becattini, Eur. Phys.J. C 77, 213 (2017).
- [4] J. Adam et al., (STAR Collaboration), Phys. Rev. C 98, 014910 (2018).
- [5] S. Alzhrani, S. Ryu, and C. Shen, Phys. Rev. C 106, 014905 (2022).
- [6] B. C. Fu, et al., Phys. Rev. Lett. 127, 142301 (2021).
- [7] J. Adam et al., (STAR Collaboration), Phys. Rev. Lett. 123, 132301(2019)
- [8] S. Acharya et al., (ALICE Collaboration), arXiv:2107.11183.